THEORETICAL ANALYSIS AND EXPERIMENTAL RESEARCH OF HEAT PUMP DRIVING HEAT PIPES HEATING EQUIPMENT

by

Ruochen DING[a,b], Baorui DU[a*], Shuxue XU[c], Jun YAO[a], and Huilong ZHENG[a]

[a] Institute of Engineering Thermophysics, Chinese Academy of Sciences, Beijing, China
[b] University of Chinese Academy of Sciences, Beijing, China
[c] College of Environmental and Energy Engineering, Beijing University of Technology, Beijing, China

Original scientific paper
https://doi.org/10.2298/TSCI190223329D

In this study, the main design parameters of the heat pump/heat pipe composite system were calculated. The operation characteristics of the heat pump/heat pipe composite system under low temperature were experimentally studied. The start-up character of the heat pipe radiator and heat pipe radiator surface temperature distribution were obtained. The variation of heating capacity and heating coefficient of performaance of the heat pump/heat pipe composite system with different working condition was obtained. Experimental results show that the heat pump/heat pipe composite system can operate efficiently and steadily when the outdoor temperature is –20~5 °C, and meet the winter heating demand in cold areas.

Key words: *heat pump, heat pipes radiator, heating coefficient of performance*

Introduction

Nowadays, the energy crisis and environmental problems are becoming more and more serious. Since 2012, China has been suffering severe smog and haze pollution, the high concentration of particulate matter (PM) 2.5 has attracted considerable attention in China. Coal consumption is responsible for 22.4% of the PM 2.5 concentration in Beijing [1]. Coal consumption in rural Beijing is used for space heating, with considerable pollution being generated from residential sectors due to incomplete coal combustion. Although the share of electricity generated from coal sources more than 65.2%, but coal in the power plant can be effectively burned and the exhaust after treatment can decrease pollution [2]. To previous problems, a switch in household energy sources from coal to electricity was advocated in rural Beijing. The government plans to broadly promote air source heat pump equipment, which has been proved be effective in many aspects of rural life. The heat pump system works by means of the vapor compression cycle, which can absorb heat from the circumstance and release heat to room during the refrigerant change phases and it has recognized as one of the most efficient heating systems [3, 4]. In China, the heat pump system is usually designed using water to carry heat and transfer heat to the air in domestic room though radiator. However, there are some problems in the application of the system, such as the water pipes are very easy to freeze and burst when the temperature is low in winter, the water circulation system is complicated and it is difficult

* Corresponding author, e-mail: dubaorui@iet.cn

to installation and maintenance. Compared with the conventional radiator heating based on convection heat emission, radiant heating has the advantages of better comfort, uniform indoor temperature distribution, and convenient maintenance.

The heat pipe is a simple device of very high thermal conductivity with no moving parts that can transport large quantities of heat efficiently fundamentally at invariable temperature without requiring any external electricity input. Heat pipes radiator was widely used in electronics, electrical and mechanical, nuclear industry, thermal engineering, construction, medical treatment, waste heat recovery, solar energy and other fields [5, 6].

Tan and Zhang [2] studied the influence factors of heat pipe structure on heat transfer coefficient to enhance the heat transfer performance of the wall implanted with heat pipes. The results show that the wall implanted with heat pipes has a great energy saving potential during the heating season. Zhang *et al*. [7] studied the dynamic performance of a heat-pipe solar photovoltaic/thermal heat pump system. They established a mathematic model integrated the transient processes of solar transmission, heat transfer, fluid-flow and photovoltaic power generation appropriately. It was concluded that this system could harvest significant amount of solar heat and electricity, thus improving the solar thermal and electrical efficiencies. Robinson and Sharp [8] established a heat pipe augmented passive solar space heating system. This system was tested in a passive solar test facility during January and February of 2013. Results showed that this system contributed to increased rate of useful thermal gains to thermal storage and to the room, and decreased rate of thermal losses to ambient. El-Baky *et al*. [9] investigated the overall effectiveness of utilizing heat pipe heat exchangers for heat recovery through external air conditioning systems in buildings in order to reduce the cooling load. The findings indicated that effectiveness and heat transfer rates are increased with the increase in fresh air inlet temperature. The study also revealed that the mass-flow rate ratio has a significant effect of temperature change of fresh air and heat recovery rate is increased by approximately 85% with the increase in fresh air inlet temperature. Yau [10] studied the effect of heat pipe heat exchangers on enhanced dehumidification in HVAC systems. The results show that the heat pipe heat exchanger can significantly improve enthalpy change. Xu *et al*. [11] proposed a concept of air-source heat pump using heat pipes as heat radiator system for room heating and developed experimental apparatus with 1 hp compressor. The results showed that air-source heat pump using heat pipes as heat radiator improved the operating performance of the heat pump system under low temperature.

In this study, an experimental prototype of heat pump/heat pipe composite system was developed with 1.5 hp (rated power 1102.5 W) compressor. The heat radiator performances of the four kinds of commonly used refrigerant inside heat pipes have been experimentally investigated. The optimum kinds of refrigerant and the refrigerant mass filling ratio of heat pipes radiator has been obtained. The experiment was conducted to evaluate the heating performance of heat pump/heat pipe composite system under low temperature conditions. Comparing with other similar systems, this system possesses such advantages as: simple structure, comfortable and easy to maintain *et al.* Compared to our previous research, we tested more kinds of refrigerant and more operating conditions. The results can provide references for the use of heat pump/heat pipe composite system in cold regions.

Heat pump/heat pipe composite system

The heat pump/heat pipe composite system is shown in fig. 1. This system consists of two parts: heat pump part and heat pipes radiator part. Heat pump includes a compressor, a condenser, a throttling device, an evaporator and connecting tubes. Heat pipes radiator part includes a couple of heat pipe and a fluid collecting container. The evaporator absorbs heat from outside room and the compressor compress the vapor to a high pressure and high temperature, and then, the high pressure and high temperature vapor flow into the condenser.

As can be seen in fig. 2, the condenser was set in the fluid collecting container of heat pipe radiator, during working process, the heat in the condenser released to the heat pipes liquid refrigerant and the liquid refrigerant evaporates and become gas-liquid state flowing upside of the heat pipes. The heat pipes radiator transmits heat to the indoor room through radiation and natural-convection.

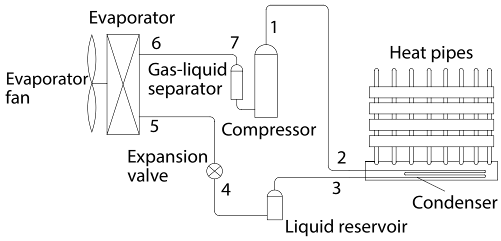

Figure 1. Heat pump/heat pipe composite system

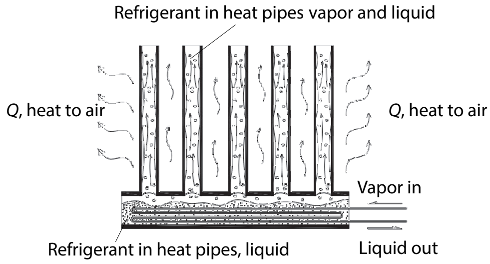

Figure 2. Heat pipes radiator and condenser

Analytical model

Heat pump working process

The high temperature and high pressure refrigerant gas discharged by the compressor enter the condenser to condense and release heat, which is transferred to the indoor environment through the heat pipes radiator. The heat transfer from the radiator to the indoor environment can be obtained by the refrigerant flow rate in the condenser and the enthalpy difference between the refrigerant inlet and outlet of the condenser. The heat emission (heating capacity, Q) from radiator to the indoor environment may be determined from the following formulation [12]:

$$Q = \dot{m}\left(h_2 - h_3\right) \tag{1}$$

where $\dot{m}$ [kgs^{-1}] is refrigerant flow rate throw condenser, h_2, h_3 [kJkg^{-1}] are the enthalpy of the data points 2 and 3 in fig. 1.

Heating COP [13]:

$$COP = \frac{Q}{P} \tag{2}$$

where P [kW] is compressor power input.

Heat emission by convection and radiation

Heat emitted from radiator through two main process, convection and radiation. Research results indicated that, much of the heat delivered to the space is by natural-convection [14]. Convection heat transfer can be determined as:

$$Q_c = h_c A\left(t_f - t_{\text{room}}\right) \tag{3}$$

where Q_c [kW] is the convective heat output, A [m^2] – the surface area, h_c [kWm^{-2}°C^{-1}] – the convection coefficient, t_f [°C] – the heat pipes radiator surface temperature, t_{room} – the room temperature.

The value of h_c can be determined as:

$$h_c = 1.31\left(\theta\right)^{0.33} \tag{4}$$

where θ [°C] is temperature difference between radiator surface and room air.

Radiation heat output can be determined as:

$$Q_r = A\varepsilon\sigma\left(t_f^4 - t_{\text{room}}^4\right) \tag{5}$$

where $\varepsilon = 0.9$, $\sigma = 5.6703 \cdot 10^{-8}$ [Wm^{-2}K^{-4}], A [m^2] – the surface area, t_f [°C] – the surface temperature of the heat pipes.

Matching of heat pump and heat pipes radiator

In order to match the heat emission of the heat pipes radiator and the heating capacity of the heat pump, the heat emission of the heat pipes radiator composed of 20 to 60 heat pipes was calculated. As shown in fig. 3, different number of heat pipe should be selected under different working conditions. Under the conditions of evaporating temperature –5 °C and condensing temperature 35 °C, the number of heat pipe matching the heat load of the compressor is 30, 35, and 40. Under these number of heat pipes, the heat generated by the heat pump can be dissipated through the heat pipes radiator, and the cost is not too high due to the excessive radiator area.

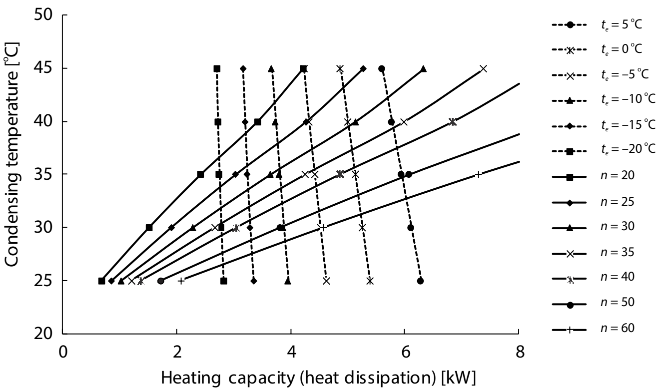

Figure 3. Heat emission of heat pipe radiator and heating capacity of compressor

Figure 3 shows the performance of heat pipes heat dissipation combined with heat pump. The solid line is heat dissipation of heat pipes radiator with different number of heat pipe under different condensation temperature. The dotted line is the heating capacity of the heat pump under different working conditions. The intersection point of the dotted line and the solid line is the working point of the system. As the condensation temperature increases, the heat dissipation of the heat pipes radiator increases, and the heating capacity of the heat pump decreases. The intersection of the heat pipes heat dissipation curve and the heat pump heating capacity curve is the best match point of the system.

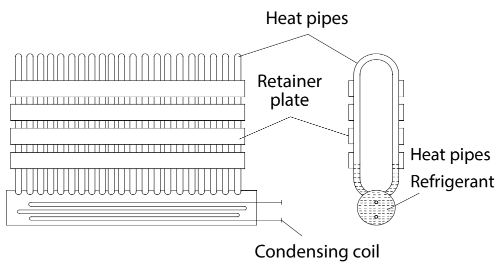

Figure 4. The structure of the evaporative condenser

Design calculation of evaporative condenser

The structure of the evaporative condenser is shown in fig. 4. The outer part is the casing (collecting liquid pipe), and the inside is the tube bundle (condensing coil). The high temperature and high pressure refrigerant vapor discharged from the compressor enters the coil to transfer heat to another refrigerant outside the condensing coil. In this process, the heat pipes radiator and the heat pump system are combined by the condensing coil, and the condensing coil is made of copper tube with a diameter of 9 mm. The heat exchange mode inside the condensing coil is in-tube condensation heat transfer, and the outside of the condensing coil is boiling heat transfer [15].

The coefficient of condensation heat transfer in the whole pipe surface area is [16]:

$$\alpha = 0.555\left[\frac{\beta}{(T_S - T_W)d}\right]^{0.25} \tag{6}$$

$$\beta = \frac{\lambda^3\rho^2 g\gamma}{\mu} \tag{7}$$

where T_S [°C] *i*s the saturation temperature of the heat pump working fluid, T_W [°C] – the average temperature of the heat pipes radiator surface, d [m] – the inner diameter of the condensing coil, λ [Wm^{-1}K^{-1}] – the thermal conductivity of the working fluid, ρ [kgm^{-3}] – the density of refrigerant, g [ms^{-2}] – the gravitational acceleration, γ [Jkg^{-1}] – the latent heat of condensation, μ [Pa·s] – the dynamic viscosity of refrigerant, physical property parameters are calculated according to the state of inlet steam.

The boiling heat transfer:

$$\mathrm{Nu} = \mathrm{Nu}_b + \mathrm{Nu}_{cv} \tag{8}$$

In the aforementioned formula, the first term is the boiling component, and the second term is the macroscopic convection component. The correlation calculation of each term is as shown in eqs. (9) and (10):

$$\mathrm{Nu}_b = \left[\frac{\mathrm{Re}_b}{\mathrm{Pr}}\left(1 - \frac{V_o^{\,m}\mathrm{Nu}_{cv}}{\mathrm{Nu}}\right)\right]^{0.7}\left(\frac{D}{B}\right)^{0.3} \tag{9}$$

$$\mathrm{Nu}_{cv} = V_o^{\,0.63}\mathrm{Nu}_L \tag{10}$$

$$\mathrm{Nu}_L = 0.27\left(\mathrm{Re}_L\right)^{0.63}\left(\mathrm{Pr}\right)^{0.36} \tag{11}$$

$$\mathrm{Re}_L = \frac{G(1-x)D}{\mu_L} \tag{12}$$

$$V_o = \frac{1}{1-\alpha} \tag{13}$$

$$\alpha = \frac{1}{1 + \left[\dfrac{1-x}{x}\right]\dfrac{\rho_G}{\rho_L}} \tag{14}$$

$$h_o = \frac{\mathrm{Nu}\lambda}{D} \tag{15}$$

where Re_b is the boiling flow Reynolds number of the fluid, Pr – the Prandtl number, V_o – the bubble parameter, D [m] – the outer diameter of the condensing coil tube, B – the constant, G [kgm^{-2}s^{-1}] – the mass flux, x – the refrigerant dryness, μ_L [Pa·s] – the liquid viscosity of refrigerant, ρ_G [kgm^{-3}] – the gas density of refrigerant, and ρ_L [kgm^{-3}] – the liquid density of refrigerant.

The thermal resistance through the condensing coil:

$$r = \frac{\delta}{\lambda} \tag{16}$$

where δ [m] is the thickness of the condensing coil tube wall, λ [Wm^{-1}K^{-1}] – the thermal conductivity of the condensing coil tube wall.

The total heat transfer coefficient of the condensing coil:

$$k = \frac{1}{\dfrac{1}{\alpha} + \dfrac{\delta}{\lambda} + \dfrac{1}{h_o}} \tag{17}$$

The heat transfer temperature difference of the condensing coil:

$$\Delta T = \frac{\left(T_{\mathrm{in}} + T_{\mathrm{out}}\right)}{2} - T_S \tag{18}$$

The condensing coil area:

$$A = \frac{Q}{k\Delta T} \tag{19}$$

It is known that the diameter of the condensing coil is 9 mm, and the single pass length is l = 1.2 m. From this, it can be concluded that the number of tubes of the condensing coil in the collecting tube:

$$n = \frac{A}{\pi dl} \tag{20}$$

It can be determined that the number of tubes is 14 and the refrigerant can be sufficiently condensed in the condenser to transfer heat to the heat pipe radiator.

According to previous analysis, an absolute new heat pipes radiator (based on 1.5 hp compressor) for room heating was preliminary designed and its main structural dimension was given in tab. 1. The parameters of each part of the system are shown in tab. 2.

Table 1. Main structural dimension of heat pipes radiator

Width [mm]	High [mm]	Thickness [mm]	Diameter [mm]	*n*
1200	800	200	16	35

Table 2. Parameters of each part of the system

Part number	Part name	Parameter
1	Compressor	1.5 hp rolling piston compressor
2	Heat pipes radiator	Shown in tab. 1
3	Electromagnetic valve	Danfoss EKA-164A
4	Evaporator	5 kW
5	Accumulator	2 L

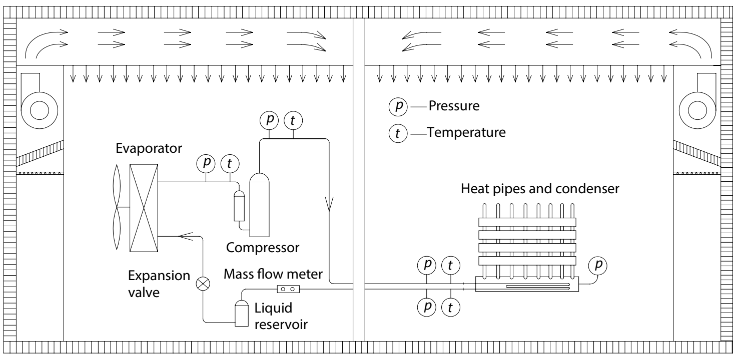

Figure 5. Schematic diagram of the experimental set-up

Experimental device

The heat pump/heat pipe composite system ex periment was conducted in the enthalpy difference room. The enthalpy difference room is divided into control room, indoor and outdoor chambers (temperature can be controlled from –20-50 °C), as shown in fig. 5.

In the experimental set-up system, the air side inlet and outlet temperature and humidity could be measured using a temperature transducer (Pt100) and a humidity transducer. Refrigerant pressures in heat pump and heat pipes were measured by pressure transducers with an uncertainty of ±0.5%. Temperatures are measured using Pt100 temperature transducer with an uncertainty of ±0.15 °C. A mass-flow meter is installed to measure the mass-flow of the refrigerant throw condenser. Power input of compressor was measured by a power meter with an uncertainty of ±0.5%.

From eqs. (1) and (2):

$$COP = \frac{Q}{P} = \frac{\dot{m}\left(h_2 - h_3\right)}{P} = f\left(m, p_2, t_2, p_3, t_3, P\right) \tag{21}$$

– first, calculate the uncertainty of each parameter, u_m, u_{t2}, u_{t3}, u_{p2}, u_{p3} u_P,
– second, calculate the combined standard uncertainty:

$$u_Q = \sqrt{\left(\frac{\partial f}{\partial \dot{m}} u_m\right)^2 + \left(\frac{\partial f}{\partial t_2} u_{t_2}\right)^2 + \left(\frac{\partial f}{\partial t_3} u_{t3}\right)^2 + \left(\frac{\partial f}{\partial p_2} u_{p_2}\right)^2 + \left(\frac{\partial f}{\partial p_3} u_{p3}\right)^2} \tag{22}$$

$$u_{\mathrm{COP}} = \sqrt{\left(\frac{\partial f}{\partial \dot{m}} u_m\right)^2 + \left(\frac{\partial f}{\partial t_2} u_{t_2}\right)^2 + \left(\frac{\partial f}{\partial t_3} u_{t3}\right)^2 + \left(\frac{\partial f}{\partial p_2} u_{p_2}\right)^2 + \left(\frac{\partial f}{\partial p_3} u_{p3}\right)^2 + \left(\frac{\partial f}{\partial P} u_P\right)^2} \tag{23}$$

– third, calculate the related expanded uncertainties (expanded factor = 2):

$$u_{\mathrm{rel},Q} = \frac{u_Q}{Q}, \quad u_{\mathrm{rel,COP}} = \frac{u_{\mathrm{COP}}}{COP} \tag{24}$$

Table 3 shows the type and accuracy of the sensor used in the experiment, and the uncertainty of the heating capacity and heating COP have been calculated out. Refrigerant mass-flow rate of heat pump system was measured by a flow meter with range of 0-150 g/s and an accuracy of ±0.2% of full scale. The variations of the measured temperature and pressure were within ± 0.15 °C and an accuracy of ±0.5%, respectively. The change of the measured compressor power input was within an accuracy of ±0.5% of full scale. When the prototype was steadily running for more than 1 hour under the selected operating mode, all measured data were recorded only if their fluctuation was within 2%.

Table 3. Uncertainties of experimental parameters

Sensor	Accuracy	Full scale	Model
Temperature	±0.15 °C	–	Pt100
Pressure transducer	±0.5% of full scale	4.0 MPa	Huba
Flow meter	±0.2% of full scale	150 gs^{-1}	Coriolis mass-flowmeter
Power acquisition unit	±0.5% of full scale	10 kW	Electrical energy tester
Data logger	±0.2% of full scale	–	Data collecting instrument
Heating capacity	2.9%		
Heating COP	3.9%		

Experimental results and discussion

The heat pipes surface temperature, heating capacity, power input and heating COP of the heat pump/heat pipe composite system were obtained through experiments. All the following investigations were undertaken under the condition: indoor temperature, t_i from 16-24 °C, outdoor temperature, t_o from –20-5 °C and the heat pump system is filled with R410A.

Heat pump/heat pipe composite system starting process

Figure 6 shows the starting processes of the heat pump/heat pipe composite system when the heat pipes radiator is filled with R32. The $t_{k,pump}$ means the condensing temperature of heat pump and $t_{k,pipe}$ means the average temperatures of heat pipes surface. Figure 6 show that, the heat pump condensing temperature increases rapidly from 20-40 °C in 30 minutes owing to the power input of heat pump. With a temperature increase of heat pump condenser, saturation temperature of the heat pipes radiator continuously increase and temperature gradient between the heat pipes saturation temperature and heat pump condensing temperature gradually reduces in 30 minutes. At the steady-state, the difference between $t_{k,pump}$ and $t_{k,pipe}$ keeps steady. After reaching the steady-state, the temperature difference between $t_{k,pump}$ and $t_{k,pipe}$ is only 1-1.5 °C.

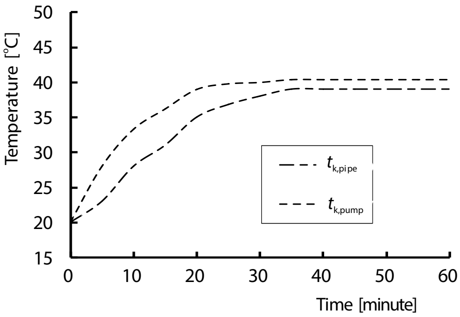

Figure 6. Starting processes of heat pump/ heat pipe composite system

The surface temperature distribution of heat pipes radiator

In order to investigate the temperature distribution on heat pipes surface, 15 temperature sensors (Pt100) are distributed evenly on the surface of heat pipes radiator and their positions are shown in fig. 7. The data of temperatures were recorded by data collection instrument.

Figure 8 shows the surface temperature distribution of heat pipes radiator surface under different working conditions when the outdoor temperature is –20 °C, –15 °C, –10 °C, –5 °C, 0 °C, 5 °C, and the indoor temperature is 20 °C. The t_1~t_{15} is the temperature of 15 temperature sensor points on the surface of the heat pipe radiator. Figure 8 show that, the lower the outdoor temperature is, the lower the heat pipes radiator surface temperature is and the lower the surface temperature of the heat pipes radiator and the surface temperature distribution of the heat pipes radiator is more uniform. For one outdoor temperature, the difference between biggest and smallest temperature was less than 2 °C. Testing results show that, heat pipes radi-

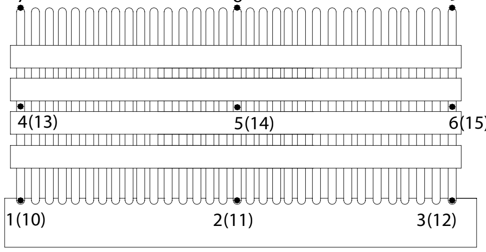

Figure 7. Position of temperature sensor on heat pipes radiator

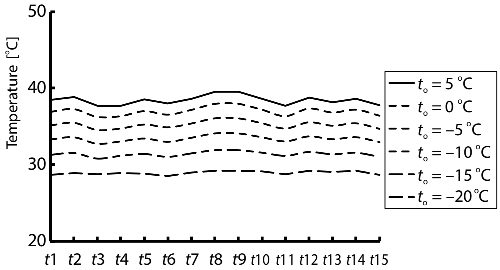

Figure 8. Temperature distribution of heat pipes radiator surface

ator is capable of producing a good uniformity for surface temperature distribution and it can effectively radiate heat to the surrounding environment.

Power input of compressor

In order to investigate the influence of different working fluids on system performance, several commonly used working fluids were selected for experiments, there were R22, R32, R134a, and R410A. These working fluids are widely used in domestic and commercial refrigeration and air conditioning equipment, very easy to be obtained.

Figure 9 shows the variation of power input of compressor with different outdoor temperature when the indoor temperature is 20 °C. The power of the compressor is collected by power acquisition unit. As can be seen from the fig. 9, the power input of compressor increases with the outdoor temperature. Under the same working condition, the minimum power input is obtained when the heat pipe radiator is filled with R32, and the maximum power input is obtained when the heat pipe radiator is filled with R410A.

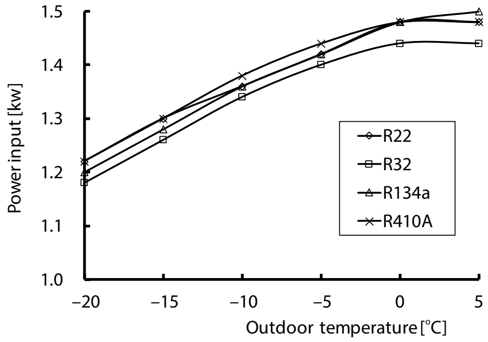

Figure 9. Variation of power input of compressor with different outdoor temperature

Heating performance under different outdoor temperature

Figure 10 shows the variation of heating capacity with different outdoor temperature. The heating capacity of heat pump is obtained by eq. (1), Where m is collected by flow meter and h_2, h_3 are calculated by refrigerant properties query software based on temperature and pressure. Heating capacity of the heat pump increases with the increase of outdoor temperature, when the heat pipes radiator filled with different working fluids, the system heating capacity is different under the same working condition. Under the same working condition, the maximum heating capacity was obtained when the heat pipe radiator is filled with R134a, and the minimum heating capacity was obtained when the heat pipe radiator is filled with R22. When the heat pipes radiator filled with R134a, the system heating capacity is about 5% higher than that the heat pipe radiator filled with R22.

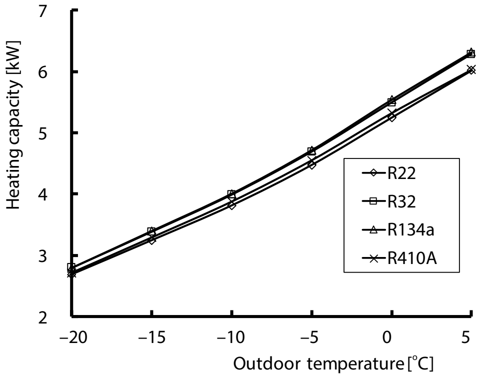

Figure 10. Variation of system heating capacity with different outdoor temperature

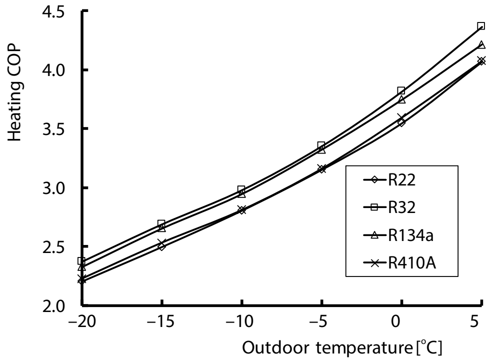

Figure 11. Variation of system heating COP with different outdoor temperature

Figure 11 shows the variation of heating COP with different outdoor temperature, heating COP increases with the increase of outdoor temperature, when the heat pipes radiator filled with different working fluids, the system heating COP is different under the same working condition. Under the same working condition, the maximum heating COP was obtained when the heat pipe radiator is filled with R32, and the minimum heating COP was obtained when the heat pipe radiator is filled with R22. When the heat pipe radiator filled with R32, the system heating capacity is about 7% higher than that the heat pipe radiator filled with R22.

Conclusions

The operation characteristics of the heat pump/heat pipe composite system under low temperature were studied, the working characteristics of heat pump and heat pipes heat radiator were experimentally researched. Heat radiator performances with different kinds of refrigerant and different refrigerant mass filling ratio of heat pipe have been experimentally investigated. The best working fluid and optimum working fluid mass filling ratio and the start-up characteristic curve of the heat pipe radiator were obtained. The rule of heating capacity and heating COP of the heat pump/heat pipe composite system was obtained. The most important conclusions of this work.

- The experimental results show that the heat pump/heat pipe composite system can operate efficiently and steadily when the outdoor temperature is –20~5 °C, and meet the winter heating demand in cold areas.
- The heat pump/heat pipe composite system can reach to stable running condition from start-up in 30 minutes.
- Heat pipes radiator is capable of producing a good uniformity for surface temperature distribution, the difference between highest and lowest temperature value was less than 1.5 °C.
- The temperature difference between condensing temperature and heat pipes surface temperature is less than 2 °C, and so, the heat pump/heat pipe composite system can achieve the highest heating capacity when the heat pipes radiator filled with R134a and the system obtain the highest heating COP when the heat pipes radiator filled with R32.

Acknowledgment

This work was supported by the National Science and Technology Leading Talents Project of 'Ten Thousand People Plan' (Y71Z01BBA1) and the Young Top-Notch Talents Team Program of Beijing Excellent Talents Funding (2017000026833TD02).

Nomenclature

A – surface area of radiator, [m^2]
D – outer diameter of the condensing coil tube, [m]
d – inner diameter of the condensing coil, [m]
G – mass flux, [kgm^{-2}s^{-1}]
g – acceleration due to gravity, [ms^{-2}]
h – enthalpy, [kJkg^{-1}]
h_c – convection coefficient, [Wm^{-2}°C^{-1}]
l – characteristic dimension, [m]
$\dot{m}$ – mass-flow rate, [kgs^{-1}]
P – power input, [kW]
p – pressure, [MPa]
Pr – Prandtl number
Q – heating capacity, [kW]
Q_c – convective heat output, [kW]
Q_r – radiation heat output, [kW]
Re_b – boiling flow Reynolds number of the fluid
T_S – saturation temperature of the heat pump working fluid, [°C]
T_W – average temperature of the heat pipes radiator surface, [°C]
t – temperature, [°C]
t_f – heat pipes radiator surface temperature, [°C]
t_{room} – room temperature, [°C]
V_o – bubble parameter
x – refrigerant dryness

Greek symbols

β – coefficient of cubical expansion
γ – latent heat of condensation, [Jkg^{-1}]
θ – temperature difference, [°C]
δ – thickness of the condensing coil tube wall, [m]
λ – thermal conductivity of the condensing coil tube wall, [$Wm^{-1}K^{-1}$]
μ – dynamic viscosity of refrigerant, [$Pa\cdot s^{-1}$]
μ_L – liquid viscosity of refrigerant, [$Pa\cdot s^{-1}$]
ρ – density of refrigerant, [kgm^{-3}]
ρ_G – gas density of refrigerant, [kgm^{-3}]
ρ_L – liquid density of refrigerant, [kgm^{-3}]

References

[1] Li, L., *et al.*, Evaluation of Future Energy Consumption on PM2.5 Emissions and Public Health Economic Loss in Beijing, *Journal of Cleaner Production*, *187* (2018), 6, pp. 1115-1128
[2] Tan, R. H., Zhang, Z. G., Heat Pipe Structure on Heat Transfer and Energy Saving Performance of the Wall Implanted with Heat Pipes during the Heating Season, *Applied Thermal Engineering*, *102* (2016), 6, pp. 633-640
[3] Nyers, J., An Analytical Method for Defining the Pump's Power Optimum of a Water-to-Water Heat Pump Heating System Using COP, *Thermal Science*, *21* (2017), 5, pp. 1999-2010
[4] Schellenberg, C., *et al*., Operational Optimisation of a Heat Pump System with Sensible Thermal Energy Storage Using Genetic Algorithm, *Thermal Science*, *22* (2018), 5, pp. 2189-2202
[5] Zhang, H. F., Chen, Y. L., A Heat Pipe Solar Collector System for Winter Heating in Zhengzhou City, China, *Thermal Science*, *21* (2017), 4, pp. 1771-1776
[6] Zhao, C. W., Zhu, X. P., Comparison of Heat Transfer Efficiency between Heat Pipe and Tube Bundles Heat Exchanger, *Thermal Science*, *19* (2015), 4, pp. 1397-1402
[7] Zhang, X., *et al.*, Dynamic Performance of Novel Solar Photo-Voltaic/Loop-Heat-Pipe Heat Pump System, *Apply Energy*, *114* (2014), 2, pp. 335-352
[8] Robinson, B. S., Sharp, M. K., Heating Season Performance Improvements for a Solar Heat Pipe System, *Solar Energy*, *110* (2014), 12, pp. 39-49
[9] El-Baky, *et al*., Heat Pipe Heat Exchanger for Heat Recovery in Air Conditioning, Applied Thermal En*gineering*, *27* (2007), 4, pp. 795-801
[10] Yau, Y. H., Analysis of Enthalpy Change with/without a Heat Pipe Heat Exchanger in a Tropical Air Conditioning System, *International Journal of Energy Research*, *30* (2006), 12, pp. 1251-1263
[11] Xu, S. X., *et al*., Investigation of Air-Source Heat Pump Using Heat Pipes as Heat Radiator, *International Journal of Refrigeration*, *90* (2018), 6, pp. 91-98
[12] Zeng, D. L., *et al.*, *Engineering Thermodynamics*, Higher Education Press, Beijing, China, 2002
[13] Cenejac, A. R., *et al*., Covering of Heat Load of Object by Using Ground Heat as a Renewable Energy Source, *Thermal Science*, *16* (2012), 1, pp. 225-235
[14] Wadowski, T., *et al.*, Characteristics of a Gravity-Assisted Heat Pipe-Based Heat Exchanger, *Heat Recovery Systems and CHP*, *11* (1991), 1, pp. 69-77
[15] Aydar, E., Ekmekci, I., Thermal Efficiency Estimation of Panel Type Radiator with CFD Analysis, *Journal of Thermal Sciences and Technology*, *32* (2012), 2, pp. 63-71
[16] Leonard, L. V., Heat Pipes in Modern Heat Exchangers, *Applied Thermal Engineering*, *25* (2005), 1, pp. 1-19

Paper submitted: February 23, 2019
Paper revised: May 3, 2019
Paper accepted: August 11, 2019